

Journal of Materials Chemistry A

Accepted Manuscript



This is an *Accepted Manuscript*, which has been through the Royal Society of Chemistry peer review process and has been accepted for publication.

Accepted Manuscripts are published online shortly after acceptance, before technical editing, formatting and proof reading. Using this free service, authors can make their results available to the community, in citable form, before we publish the edited article. We will replace this *Accepted Manuscript* with the edited and formatted *Advance Article* as soon as it is available.

You can find more information about *Accepted Manuscripts* in the [Information for Authors](#).

Please note that technical editing may introduce minor changes to the text and/or graphics, which may alter content. The journal's standard [Terms & Conditions](#) and the [Ethical guidelines](#) still apply. In no event shall the Royal Society of Chemistry be held responsible for any errors or omissions in this *Accepted Manuscript* or any consequences arising from the use of any information it contains.

Cellulose nanocrystal-based composite electrolyte with superior dimensional stability for alkaline fuel cell membranes

Yuan Lu, Aaron A. Armentrout, Juchuan Li, Halil L. Tekinalp, Jagjit Nanda, Soydan Ozcan*

Materials Science and Technology Division, Oak Ridge National Laboratory, 1 Bethel Valley Road, Oak Ridge, Knoxville, TN. 37831

*Address correspondence to Dr. Soydan Ozcan

Email: ozcans@ornl.gov.

Abstract

Cellulose nanocrystal (CNC)-based composite films were prepared as a solid electrolyte for alkaline fuel cells. Poly (vinyl alcohol) (PVA) and silica gel hybrid was used to bind the CNCs to form a robust composite film. The mass ratio (i.e., 1 : 1, 1 : 2) of PVA and silica gel was tuned to control the hydrophobicity of the resulting films. Composite films with a range of CNC content (i.e., 20 to 60%) were prepared to demonstrate the impact of CNC on the performance of these materials as a solid electrolyte for alkaline fuel cells. Different from previously reported cross-linked polymer films, CNC-based composite films with 40% hydrophobic binder (i.e., PVA : silica gel=1 : 2) exhibited simultaneous low water swelling (e.g., ~5%) and high water uptake (e.g., ~80%) due to the hydrophilicity and extraordinary dimensional stability of CNC. It also showed a conductivity of 0.044 and 0.065 S/cm at 20 and 60 °C, respectively. To the best of our knowledge, the film with 60% CNC and 40% binder is characterized by the lowest hydroxide conductivity-normalized swelling ratio. Decreased CNC content (i.e., 40 and 20%) resulted in comparable hydroxide conductivity but a greater swelling ratio. These results demonstrate the

advantage of CNC as a key component for a solid electrolyte for alkaline fuel cells over conventional polymers, suggesting the great potential of CNCs in improving the dimensional stability while maintaining the conductivity of existing anion exchange membranes.

Introduction

Fuel cells are novel devices which convert chemical energy into electrical energy with little emissions and high efficiency.¹⁻³ Anion exchange membrane fuel cells (AEMFCs) are currently experiencing a resurgence in research interest due to superior reaction kinetics at the electrodes the use of more affordable materials, lower native operating temperatures, and intrinsically lower methanol permeability.^{4, 5} The desire for an improved anion exchange membrane (AEM) has been the focus of much of the current research into AEMFC technology, with the primary challenges being lackluster ionic conductivity and insufficient dimensional stability.⁶ However, bolstering ion conductivity in AEMs has been found to lead to excessive water uptake, with detrimental consequences in terms of dimensional stability (i.e., high swelling).⁷

Covalent cross-linking has been employed as an effective approach to reduce the water swelling of AEMs.⁸⁻¹¹ Multifunctional compounds including dithiol,⁸ dialdehyde,¹⁰ alkoxy silanes,⁹ diamines¹² and tetraepoxy¹¹ have been reported as cross-linking agents. Despite the covalent cross-linking, hydrophilic membranes (e.g., tetraalkoxy silanes-cross-linked membrane) still exhibited a swelling ratio of ~20% due to high water uptake (e.g., ~60%).⁹ Indeed, cross-linked hydrophobic membranes (e.g., poly(phenylene oxide)) showed much lower swelling (e.g., < 5%). However, they are characterized by low water uptake (e.g., ~30%), resulting in reduced ionic exchange capacity and hydroxide conductivity.¹³ As such, a strategy is still yet to be developed for simultaneous low membrane swelling and high water uptake.

Cellulose nanocrystals (CNCs) are a naturally derived biodegradable nanomaterial that has high mechanical strength, high water absorption, great wet dimensional stability, and numerous hydroxyl functional groups.^{14, 15} The extraordinary dimensional stability, along with the highly hydrophilic properties, suits CNC well as an ideal precursor for a solid electrolyte with low swelling and high water uptake. The large amount of hydroxyl groups on the CNC surface also facilitates the grafting of cations for enhanced ionic exchange capacity and conductivity. In this article, we report on the preparation of CNC-based solid electrolyte membranes using poly(vinyl alcohol) (PVA) and trimethoxy(methyl)silane as the binder for alkaline fuel cells. These films exhibited superior dimensional stability, handleability, and hydroxide conductivity. For the CNC-composite film with swelling ratio of ~5%, the water uptake (e.g., > 80%) is significantly greater compared to previously reported membranes.

Experimental

Materials

Poly (vinyl alcohol) (87-89% hydrolyzed) was purchased from Aldrich Chemistry. Trimethoxy (methyl) silane ($\geq 97.5\%$ purity) was purchased from Aldrich Chemistry. Cellulose Nanocrystals (0.94 wt% Sulfur) with typical diameter of 5–10 nm and length of 200–400 nm was acquired from the U.S. Department of Agriculture's Forest Products Laboratory. Hydrochloric Acid (6.0 N) was purchased from Alfa Aesar. Common laboratory salts and solvents were purchased from Fisher Scientific (Pittsburgh, PA). Unless noted otherwise, all materials were used as received without further purification.

Preparation of cross-linked cellulose nanocrystal PVA membrane

PVA (5 g) was dissolved in DI water (100 mL) under stirring at 85 °C in a round bottom flask equipped with a condenser. The solution was then removed and allowed to cool to room temperature. CNC (1 g) was mixed with DI water (20 mL) and sonicated for approximately 60 s until homogeneity was achieved. Xerogel synthesis was carried out by combining HCl (90 μ L), MTMOS (1136 μ L), and DI water (9766 μ L) under magnetic stirring for 15 min. Upon completion, the xerogel solution was immediately mixed with the PVA solution in a glass vial and gently swirled for approximately 20 s to form two separate homogeneous binder solutions, with binder A containing a 1 : 1 mass ratio of xerogel to PVA and binder B containing a 1 : 2 mass ratio. The binder solutions were then immediately mixed with the CNC solution in glass vials at various specific mass ratios (40 to 80%) and gently swirled for approximately 20 s. All membranes have a total mass of 500 mg excluding water. The binder-CNC solution was then immediately cast into plastic petri dishes and left to dry for 12 h. The dried membranes were then placed in the oven to cure at 40 °C for 48 h.

Characterizations of the CNC-based composite films

Water uptake was measured by first recording the dry mass of individual membrane strips. The membrane strips were then immersed individually in DI water at 20 or 60 °C. After 24 h, the strips were removed and the surface was carefully dried utilizing absorbent paper. The mass was then quickly recorded to avoid water loss during the measurement. The water uptake (WU) was calculated from:

$$WU(\%) = \frac{m_{hydrated} - m_{dry}}{m_{dry}} \times 100\%$$

Swelling degree was measured by carefully recording the dimensions of individual membrane strips (approximately 56 x 13 x 0.075mm dry). The strips were then immersed in DI water at 20

or 60 °C for 24 h. The strips were then removed and the dimensions were measured again. The swelling degree (SD) was calculated as:

$$SD(\%) = \frac{x_{hydrated} - x_{dry}}{x_{dry}} \cdot 100\%$$

Tensile testing of the wet films was carried out at room temperature (25 °C) utilizing the RSA III Rheometrics System Analyzer manufactured by TA Instruments. CNC-composite films were immersed in water for 24 h prior to the tensile testing. Rectangular geometry tensile-testing quantified stress/strain performance. Modulus was calculated by analysis of the low strain portion of the stress/strain curve.

Infrared adsorption spectra of CNC-based composite films were obtained with the attenuated total reflectance technique using a Thermo Nicolet Nexus 670 FTIR spectrometer to characterize the chemical composition of the composite films

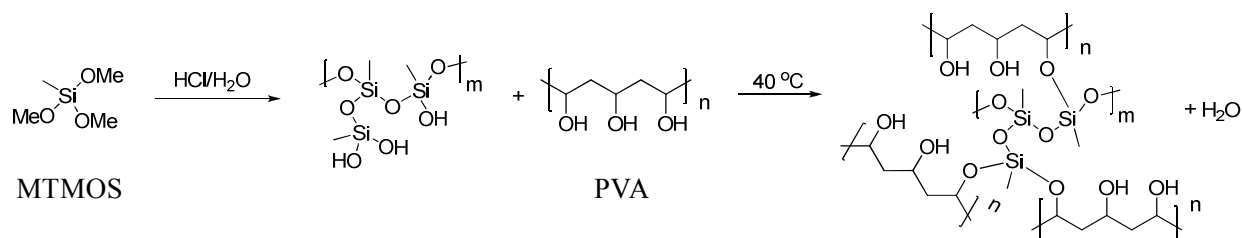
Differential scanning calorimetry (DSC) measurements were performed to characterize the change of glass transition and melting temperature resulted from the crosslinking using a TA DSC Q2000 from 20 to 300 °C, with cooling and heating rates of 10 °C/min.

Electrochemical impedance spectroscopy (EIS) was measured using a potentiostat (VSP, Bio-Logic). Specimens from at least four batches were used. The applied potential was 10 mV, and the frequency was scanned from 1 MHz to 50 mHz with 5 points per decade. A home-made Swagelok cell was used to implement the EIS measurement, and two stainless steel rods with polished surfaces were used as the electrodes. The temperature was kept constant (20 or 60 °C) during the measurement.

Results and Discussion

Synthesis of CNC-based composite films.

Cellulose nanocrystals (CNC) are known to form transparent films which disintegrate upon exposure to water, limiting its application as an electrolyte membrane for alkaline fuel cells. In this study, PVA-silica gel polymer hybrids were employed as the binder for CNC to form a stable film in water. PVA-silica gel hybrids are cross-linked networks that have been extensively studied for various applications.¹⁶ As shown in Scheme 1, silanes were first hydrolyzed and condensed to form a highly branched silica network with hydroxyl groups which further condensed with those on PVA, yielding a cross-linked network.



Scheme 1. Sol-gel chemistry to prepare PVA/silica gel polymer hybrids

Given the fact that the sol-gel chemistry is conducted in an aqueous environment, a great medium for uniform dispersion of CNC, we expect the PVA/silica gel hybrids to be ideal binders for CNC films. Hydrophobicity of the electrolyte membrane is known to play a key role in the water absorption and dimensional stability of the film. Two binders were thus prepared with different mass ratios of PVA to silane MTMOS which are 1 : 1 and 1 : 2 for binder A and B, respectively. Because MTMOS is a hydrophobic silane, binder B is characterized by greater hydrophobicity compared to binder A. To systematically study the effect of binder content on their performance as solid electrolytes for alkaline fuel cells, composite films with various CNC

content were prepared. Table 1 lists the composition of the CNC-based composite films prepared in this study.

Table 1. CNC-based composite films with PVA/silica gel binders

Film	40A	40B	60B	80B
Type of binder*	A	B	B	B
Binder content (%)	40	40	60	80
CNC content	60	60	40	20

*The ratio of PVA to silica gel is 1 : 1 and 1 : 2 for binder A and B, respectively.

FT-IR spectra of these films are shown in Figure 1. All the spectra show a large band between 3200 and 3600 cm^{-1} , which corresponds to the stretching vibration of $-\text{OH}$ groups from CNC, PVA, and silica gel. The peak at 1275 cm^{-1} was ascribed to the characteristic vibrations of C-Si asymmetric stretching in C-Si-O. Distinct peaks at 780 and 1150 cm^{-1} are from the stretching of Si-O-Si and Si-O-C, respectively. The presence of these bonds confirms the formation of a cross-linked PVA-silica gel hybrid network. Of note, the FT-IR spectrum of film 40B shows greater absorption for C-Si-O (1275 cm^{-1}), Si-O-Si (780 cm^{-1}), and Si-O-C (1150 cm^{-1}) compared to film 40A because of the higher silane content in the binder. Analogously, it is also not surprising that the intensity of these peaks increased with the binder B content.

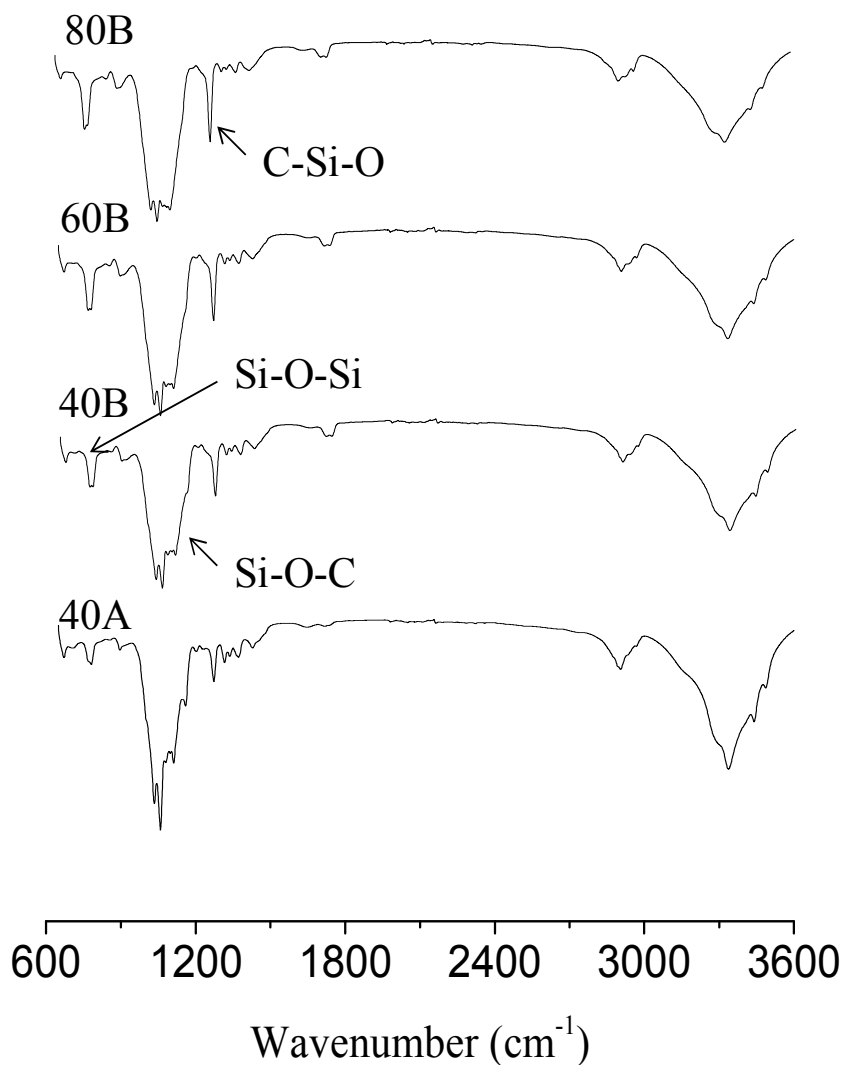


Figure 1. The FT-IR spectra of CNC-based composite films

To further confirm the formation of a cross-linked network, DSC was performed to characterize the thermal properties of the composite films. The second heating curve was used to study the glass transition of PVA in different films. Due to the presence of moisture absorbed on PVA and CNC, the glass transition of PVA is often overlapped with a broad peak of moisture evaporation in the first heating run. Therefore, the second heating curve was used to show the inherent

thermal properties of these materials. As shown in Figure 2, PVA shows a narrow glass transition range, which is expected given the homogenous chemical structure. On the contrary, a broad glass transition range can be seen on the DSC curves for the CNC-based composite films, which is attributed to the heterogeneity in chemical structure caused by the cross-linking.¹⁷

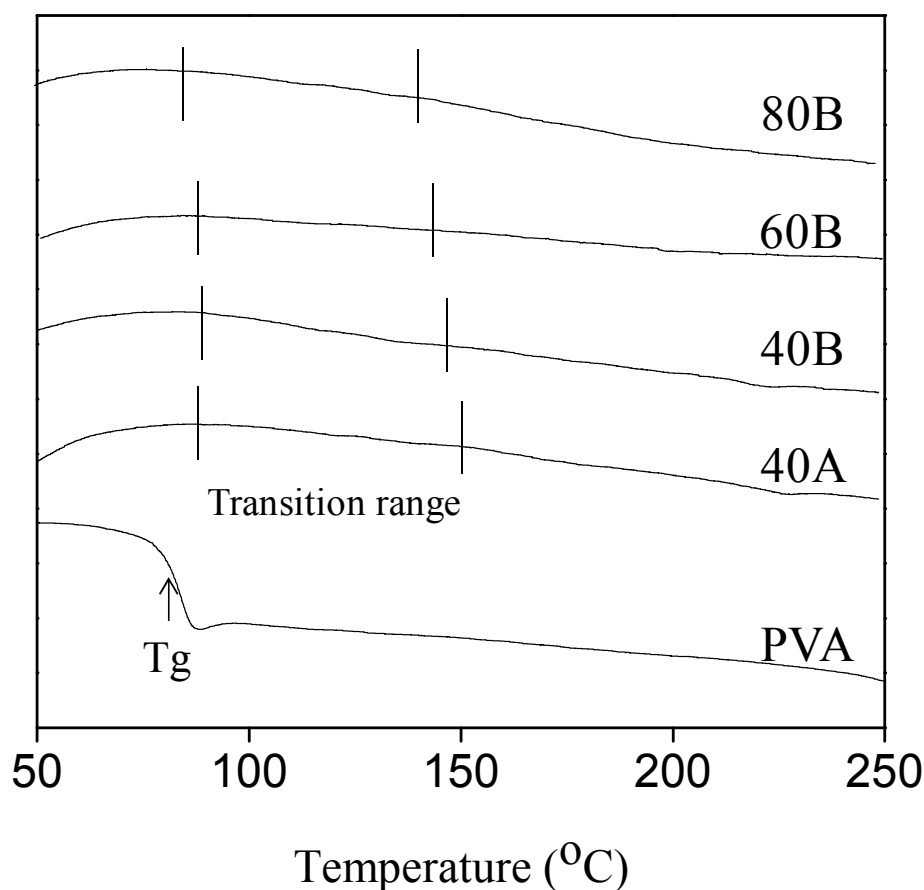


Figure 2. Glass transition for PVA and CNC-based composite films shown in the second heating curves of the DSC thermographs.

Additionally, the silane cross-linking resulted in an increased melting temperature of PVA in the CNC-composite films. Figure 3 shows the first heating curves of the DSC thermographs. The melting temperature for PVA (87-89% hydrolyzed) is around 190 °C, which is in good

agreement with the literature value.¹⁸ The melting endothermic peak shifted to higher temperatures (e.g., ~ 220 °C) for the CNC-based composite films, as a result of the reduced chain mobility by silane cross-linking.

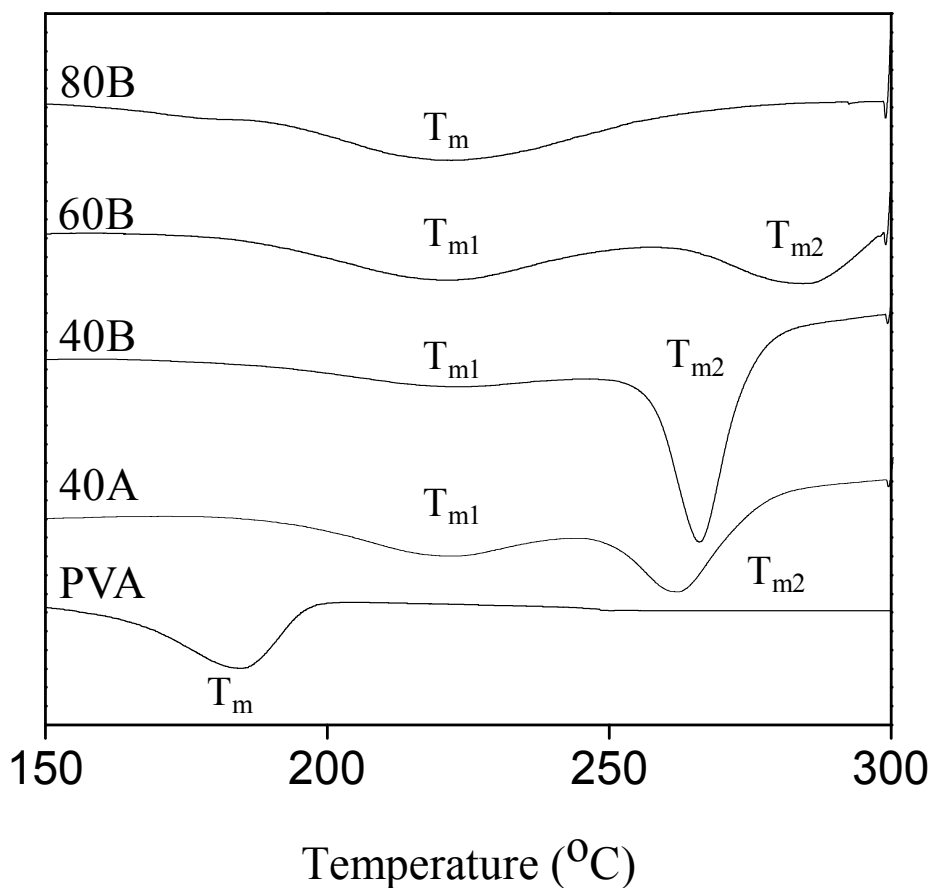


Figure 3. Melting temperatures for PVA and the CNC-based composite films shown in the first heating curves of the DSC thermographs.

Interestingly, for films with high CNC content (e.g., 40A, 40B, 60B), a second melting peak above 250 °C was observed, corroborating previous reports on PVA/nanocellulose composites.¹⁹ The intensity of this peak increases gradually with the CNC content, suggesting a crystalline

phase induced by the presence of CNC. According to Tanigami et al.,²⁰ the stereo-regularity of PVA contributes to the dual melting points and crystal phases. The lower melting point corresponds to the phase formed primarily by syndiotactic sequences, while the higher melting point is related to the phase formed primarily by atactic sequences. In this context, the addition of CNC may promote the formation of the latter crystal phase, resulting in dual melting peaks.

Water uptake and swelling

Water uptake and swelling of the CNC-based composite films were evaluated at both room temperature and 60 °C, which are commonly used as operating temperatures for alkaline fuel cells. The measurements were carried out quickly to avoid water loss. As expected, film 40A exhibited the greatest water uptake (e.g., ~160%) due to the hydrophilicity of binder A. The high water uptake led to a significant swelling ratio of ~20%, which is characteristic of PVA-based materials. In contrast, the series films using binder B exhibited much lower swelling. For example, film 40B exhibited extremely low swelling of ~5% at both temperatures as a result of the lower water uptake (~80%) compared to 40A. Further inspection of the results revealed that the swelling increases with the binder content. Compared to film 40B, the swelling of 80B increased to ~17% at both temperatures. In addition, the swelling of film 60B (i.e., ~10%) is greater than that of film 40B although both films exhibited similar water uptake. This result reveals the important role of CNC in limiting the swelling of the composite films. Indeed, nanocellulose materials are known to have high water uptake and excellent wet dimensional stability.¹⁵ Notably, when CNC content is 60% (i.e., 40B), the composite film exhibited a comparable swelling ratio but much higher water uptake when compared to the previously reported cross-linked poly(phenylene oxide) films.¹³ Greater water content in the film is known to contribute to greater hydroxide conductivity via the Grotthuss mechanism, a well-known

mechanism for hydroxide diffusion in aqueous solution.^{21, 22} These results demonstrate the advantage of CNC-based composite films in maintaining low swelling with high water uptake compared to conventional polymer membranes. Of note, the swelling was measured at both edges and center of the film. The standard deviation thus represents how isotropic of the swelling.

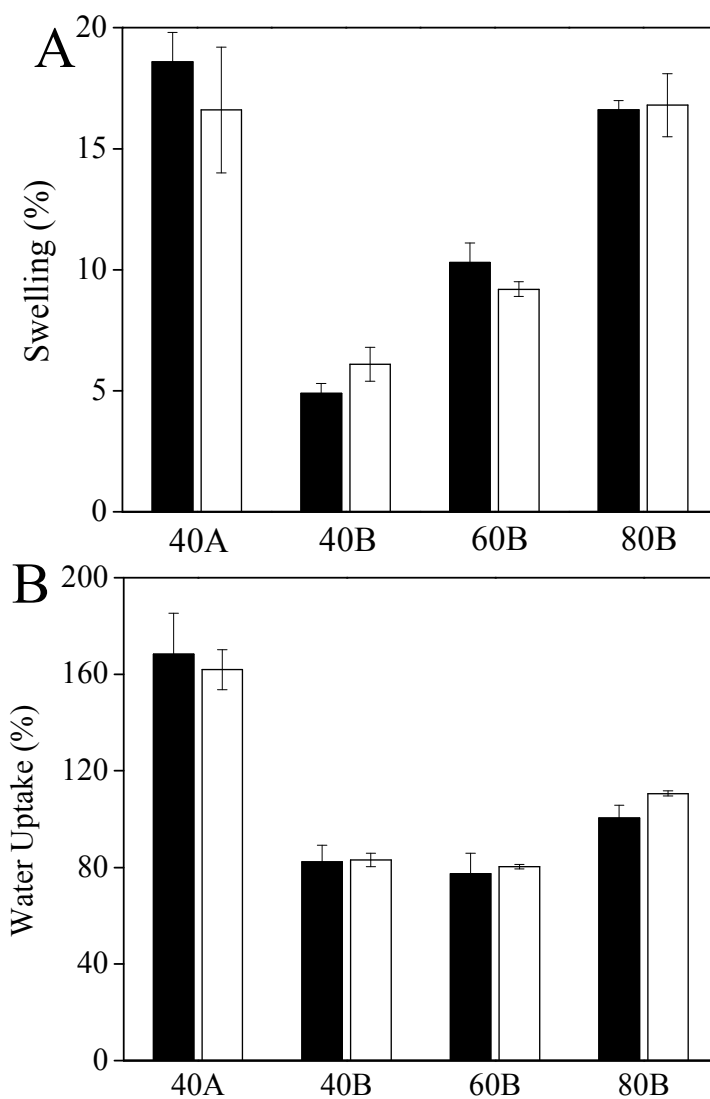


Figure 4. Water uptake and swelling of CNC-based composite films at room temperature (black) and 60 °C (white).

Mechanical properties

Tensile testing was conducted to evaluate the mechanical properties of the CNC-based composite films. All films were immersed in water for 24 h prior to the test. All measurements were conducted under ambient conditions. Since the measurements take less than 1 min, no significant change in properties is expected. Binder B series were selected to show the influence of CNC content on the mechanical properties such as tensile strength, modulus, and elongation at break. (Figure 5) Mechanical properties are an important indicator of the robustness of the films in terms of practical handling, which is a big challenge for many hydrophilic anion exchange membranes. The water absorbed by the film often results in a low modulus. Consequently, the films appear to be soft and lack a self-supporting ability.

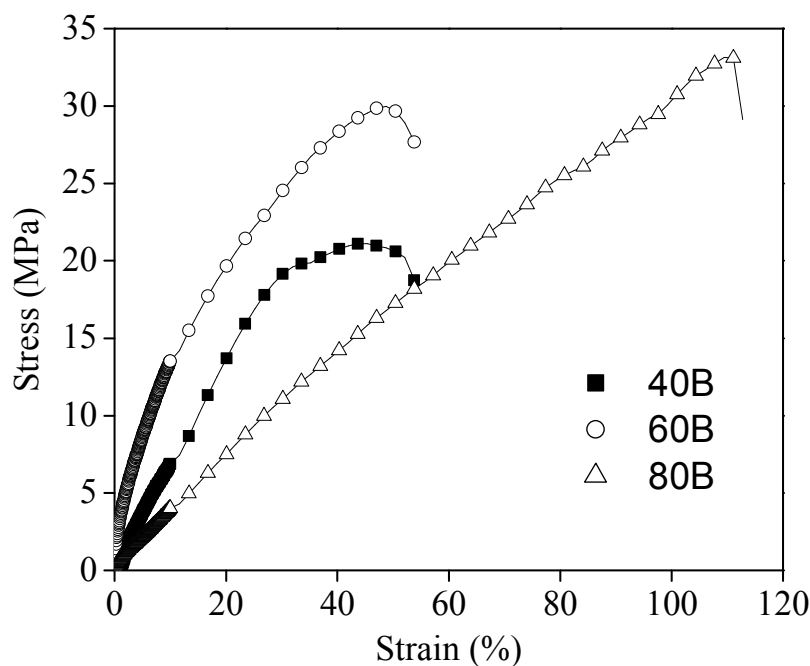


Figure 5. Stress-strain curves of CNC-based composite films.

As such, it is extremely difficult to handle these materials with ease. As shown in Figure 5 and Table 2, film 80B exhibited the lowest modulus and highest elongation as a result of the greater water uptake (e.g., ~160%) compared to film 40B and 60B. The film showed poor self-supporting ability and collapsed on itself when being lifted up. (Figure 6B) In contrast, film 40B maintained its original shape, suggesting a good self-supporting ability and handleability. (Figure 6A)

Table 2. Mechanical properties of CNC-based composite films with water uptake

Films	Tensile Strength (MPa)	Modulus (MPa)	Elongation (%)
40B	19.6 ± 1.0	65.0 ± 1.0	43.0 ± 3.5
60B	34.2 ± 4.3	129.0 ± 5.1	44.2 ± 3.8
80B	33.2 ± 0.8	31.5 ± 2.1	112.5 ± 3.5

There are two reasons for the higher modulus of film 40B and 60B. In addition to the lower water uptake (e.g., ~80%), the reinforcing effect of CNC plays an important role in enhancing the modulus. CNC has extraordinary mechanical properties and is widely used as reinforcing agent for different polymers.²³⁻³⁰ Indeed, CNC has been used to reinforce PVA, resulting in increased modulus.^{31, 32} Of note, film 40B exhibited lower tensile strength and modulus than 60B, probably a result of the lower amount of binder in the film. As mentioned earlier, pure CNC films disintegrate in water due to a lack of strong binding between individual CNCs. The use of a binder is necessary to achieve mechanical strength. Clearly, higher binder content is expected to lead to better wetting of the CNCs and the consequent enhanced mechanical properties. However, higher binder content (i.e., 60B) also contributes to increased swelling (e.g., ~10%). As such, CNC is a double-edged sword which contributes to low swelling but poor mechanical strength. Of note, the tensile strength of 40B is comparable to other previously reported anion

exchange membranes.³³ Collectively, film 40B is the most promising candidate as a solid electrolyte for alkaline fuel cells given its great dimensional stability, handleability, and water uptake.

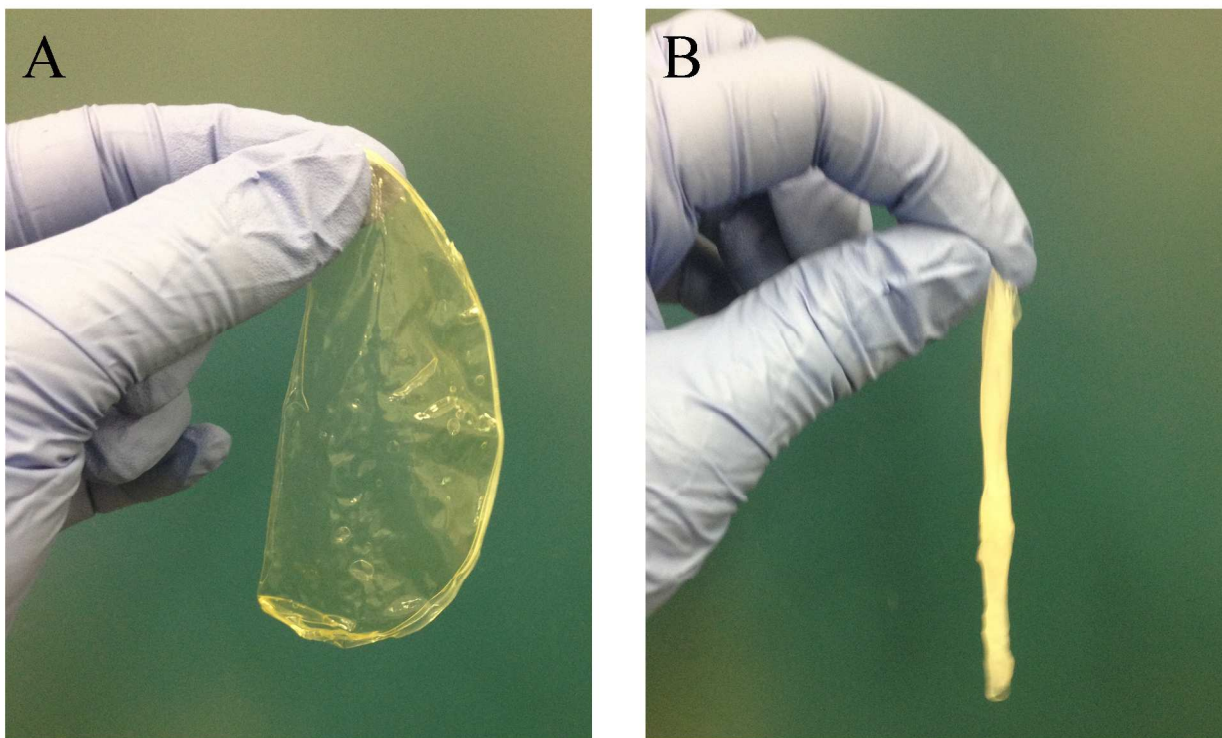


Figure 6. Digital images of wet film 40B (A) and 80B (B) showing enhanced self-supporting ability of 40B.

Hydroxide conductivity

Films 40B and 80B were selected to study the effect of CNC content on the hydroxide conductivity. The CNC-based composite films were immersed in 1 M KOH for 24 h prior to the conductivity measurements at room temperature (20 °C) and 60 °C. The hydroxide conductivity was determined to be 0.044 and 0.053 S/cm for 40B and 80B at 20 °C, respectively, comparable to previously reported cross-linked poly(phenylene oxide) films and meeting the basic

requirement for membranes in an alkaline fuel cell ($>10^{-2}$ S/cm).³⁴ Film 80B exhibited slightly greater conductivity because of the higher water uptake. However, the difference is negligible at higher temperature (i.e., 60 °C), suggesting that temperature plays a more significant role in the hydroxide conductance. Compared to a commercial FAA anion exchange membrane, which is characterized by a swelling of 17% and conductivity of 0.038 S/cm,¹³ film 40B exhibited a much lower swelling and slightly higher conductivity.

Additionally, film 40B also showed superior dimensional stability compared to some other previously reported cross-linked AEMs (e.g., commercial FAA, quaternary ammonium polysulfone, cross-linked quaternary phosphonium, quaternary ammonium poly(phenylene oxide)) as shown in Figure 8. To date, the AEM with the lowest hydroxide conductivity-normalized swelling ratio is cross-linked poly(phenylene oxide) (PPO) (0.16% cm/mS),¹³ which is higher than that for film 40B (0.11% cm/mS). These results suggest that the use of CNC-based composites is an effective strategy to achieve low swelling ratio while maintaining the ion conductivity.

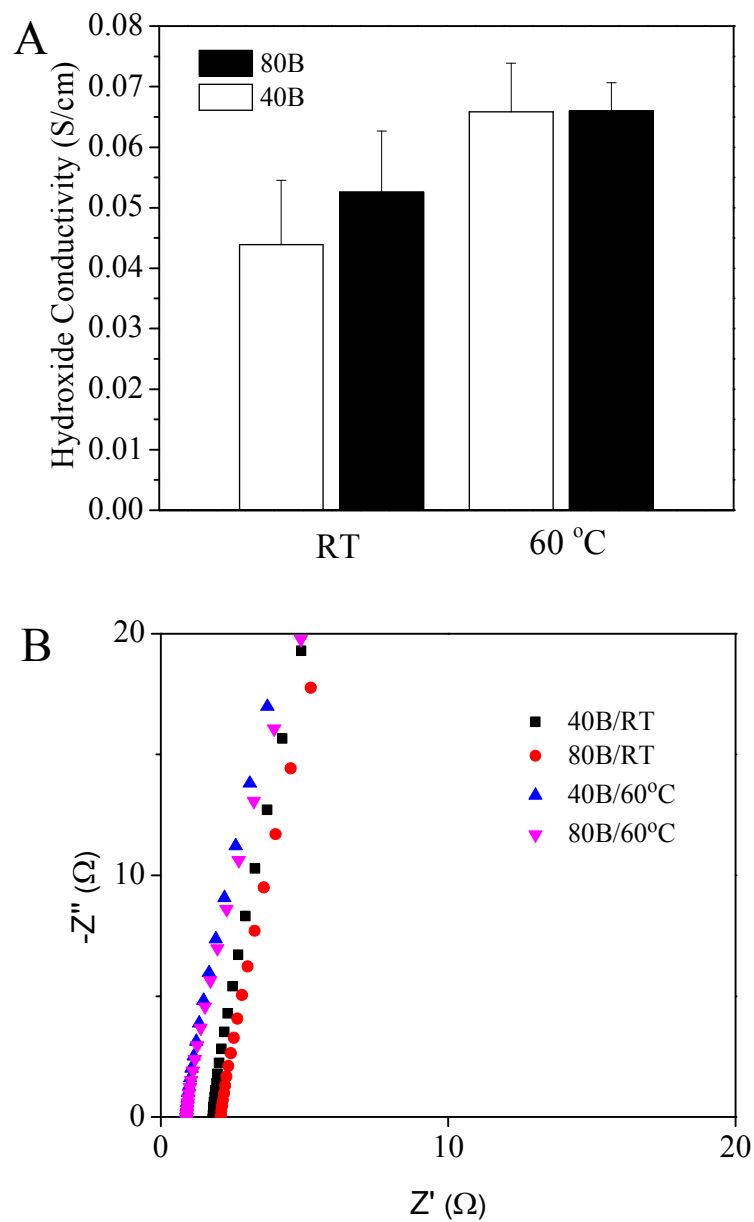


Figure 7. Hydroxide conductivity (A) and impedance spectra (B) of KOH-doped CNC-based composite films.

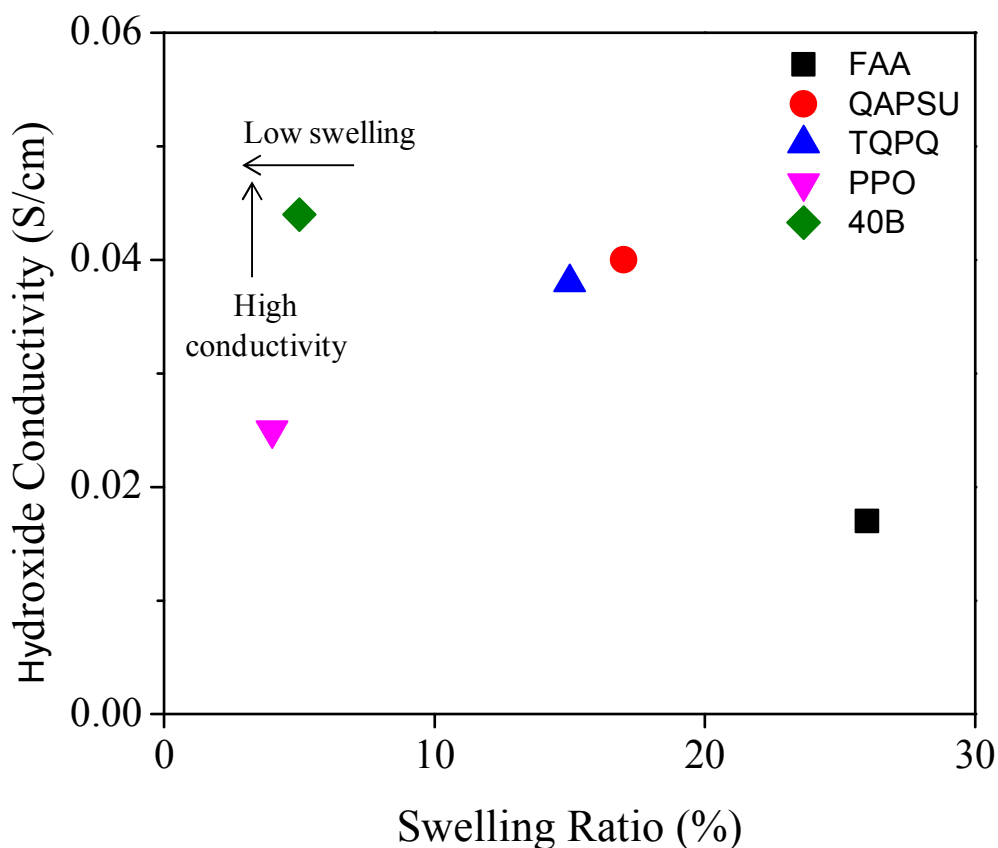


Figure 8. Comparison of hydroxide conductivity of film 40B to literature values for commercial FAA¹³ and reported chemically cross-linked AEMs (quaternary ammonium polysulfone (QAPSU),³⁵ cross-linked quaternary phosphonium (TQPQ),³⁶ and quaternary ammonium poly(phenylene oxide) (QAPPO) membranes¹³) as a function of water swelling ratio.

Conclusions

The aim of this study was to develop a strategy to design a solid electrolyte with simultaneous low swelling ratio and high water uptake for alkaline fuel cells without compromising on the conductivity. CNC-based composite films were prepared with PVA-silica gel hybrid as the binder. The hydrophobicity of the binder and CNC content were found to play an important role in the water uptake, swelling, mechanical properties and hydroxide conductivity. Composite film

40B exhibited superior dimensional stability, higher water uptake, and lower conductivity-normalized swelling ratio compared to previously-reported cross-linked AEMs.^{13,35,36} The results shown in this article demonstrate the great potential of CNC-based composite films as solid electrolytes for alkaline fuel cells. Most importantly, CNC is predicted to work well with other existing AEMs to reduce their swelling ratio. Further modification of CNC with suitable cations may result in even greater hydroxide conductivity.

Acknowledgement

The authors thank Michal Lance for his assistance in the FT-IR analysis. Thanks to the USDA Forest Service Forest Products Laboratory for providing cellulose nanomaterials as well as information on the properties of cellulosic nanomaterials. This research was sponsored by the Laboratory Directed Research and Development Program of Oak Ridge National Laboratory, managed by UT-Battelle, LLC, for the U. S. Department of Energy. This article has been authored by UT-Battelle, LLC, under Contract No. DE-AC05-00OR22725 with the US Department of Energy. The U.S. Government is authorized to reproduce and distribute reprints for Government purposes notwithstanding any copyright notation hereon.

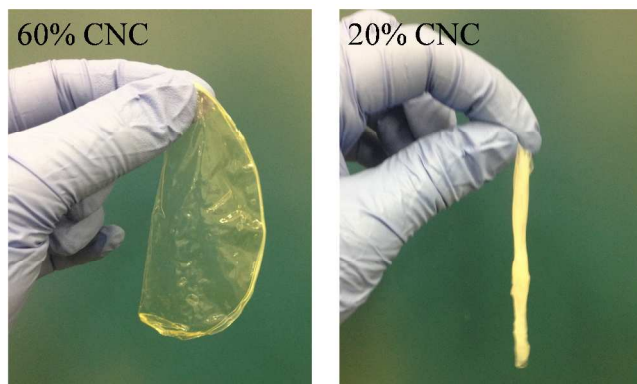
References

1. Steele, B. C. H.; Heinzl, A., *Nature* **2001**, *414*, 345-352.
2. Zhong, C. J.; Luo, J.; Njoki, P. N.; Mott, D.; Wanjala, B.; Loukrakpam, R.; Lim, S.; Wang, L.; Fang, B.; Xu, Z. C., *Energ. Environ. Sci.* **2008**, *1*, 454-466.
3. Devanathan, R., *Energ. Environ. Sci.* **2008**, *1*, 101-119.
4. Xiong, Y.; Fang, J.; Zeng, Q. H.; Liu, Q. L., *J. Membr. Sci.* **2008**, *311*, 319-325.

5. Wang, J. J.; He, G. H.; Wu, X. M.; Yan, X. M.; Zhang, Y. P.; Wang, Y. D.; Du, L., *J. Membr. Sci.* **2014**, *459*, 86-95.
6. Merle, G.; Wessling, M.; Nijmeijer, K., *J. Membr. Sci.* **2011**, *377*, 1-35.
7. Zhou, J. F.; Unlu, M.; Vega, J. A.; Kohl, P. A., *J. Power Sources* **2009**, *190*, 285-292.
8. Stoica, D.; Ogier, L.; Akrou, L.; Alloin, F.; Fauvarque, J. F., *Electrochim. Acta* **2007**, *53*, 1596-1603.
9. Wu, Y. H.; Wu, C. M.; Li, Y.; Xu, T. W.; Fu, Y. X., *J. Membr. Sci.* **2010**, *350*, 322-332.
10. Yang, C. C.; Chiu, S. J.; Chien, W. C.; Chiu, S. S., *J. Power Sources* **2010**, *195*, 2212-2219.
11. Zhou, J. F.; Unlu, M.; Anestis-Richard, I.; Kohl, P. A., *J. Membr. Sci.* **2010**, *350*, 286-292.
12. Park, J. S.; Park, S. H.; Yim, S. D.; Yoon, Y. G.; Lee, W. Y.; Kim, C. S., *J. Power Sources* **2008**, *178*, 620-626.
13. Li, N. W.; Wang, L. Z.; Hickner, M., *Chem. Commun.* **2014**, *50*, 4092-4095.
14. Habibi, Y.; Lucia, L. A.; Rojas, O. J., *Chem. Rev.* **2010**, *110*, 3479-3500.
15. Lu, Y.; Tekinalp, H. L.; Eberle, C. C.; Peter, W.; Naskar, A. K.; Ozcan, S., *Tappi J.* **2014**, *13*, 47-54.
16. Tamaki, R.; Chujo, Y., *Appl. Organomet. Chem.* **1998**, *12*, 755-762.
17. Zarzyka, I.; Pyda, M.; Di Lorenzo, M. L., *Colloid Polym. Sci.* **2014**, *292*, 485-492.
18. Peresin, M. S.; Habibi, Y.; Zoppe, J. O.; Pawlak, J. J.; Rojas, O. J., *Biomacromolecules* **2010**, *11*, 674-681.
19. Nigrawal, A.; Prajapati, S. C.; Chand, N., *J. Sci. Res. Rev.* **2012**, *50*, 40-50.

20. Tanigami, T.; Hanatani, H.; Yamaura, K.; Matsuzawa, S., *Eur. Polym. J.* **1999**, *35*, 1165-1171.
21. Jensen, M. O.; Rothlisberger, U.; Rovira, C., *Biophys. J.* **2005**, *89*, 1744-1759.
22. Grew, K. N.; Chiu, W. K. S., *J. Electrochem. Soc.* **2010**, *157*, B327-B337.
23. Xu, X. Z.; Liu, F.; Jiang, L.; Zhu, J. Y.; Haagenson, D.; Wiesenborn, D. P., *ACS Appl. Mater. Interfaces* **2013**, *5*, 2999-3009.
24. Cao, X. D.; Habibi, Y.; Lucia, L. A., *J. Mater. Chem.* **2009**, *19*, 7137-7145.
25. de Menezes, A. J.; Siqueira, G.; Curvelo, A. A. S.; Dufresne, A., *Polymer* **2009**, *50*, 4552-4563.
26. Dong, H.; Strawhecker, K. E.; Snyder, J. F.; Orlicki, J. A.; Reiner, R. S.; Rudie, A. W., *Carbohydr. Polym.* **2012**, *87*, 2488-2495.
27. Goffin, A. L.; Raquez, J. M.; Duquesne, E.; Siqueira, G.; Habibi, Y.; Dufresne, A.; Dubois, P., *Biomacromolecules* **2011**, *12*, 2456-2465.
28. Hu, X.; Xu, C.; Gao, J.; Yang, G.; Geng, C.; Chen, F.; Fu, Q., *Compos. Sci. Eng.* **2013**, *78*, 63-68.
29. Lin, N.; Dufresne, A., *Macromolecules* **2013**, *46*, 5570-5583.
30. Marcovich, N.; Auad, M.; Bellesi, N.; Nutt, S.; Aranguren, M., *J. Mater. Res.* **2006**, *21*, 870-881.
31. Lee, S. Y.; Mohan, D. J.; Kang, I. A.; Doh, G. H.; Lee, S.; Han, S. O., *Fiber Polym.* **2009**, *10*, 77-82.
32. Cho, M. J.; Park, B. D., *J. Ind. Eng. Chem.* **2011**, *17*, 36-40.
33. Ran, J.; Wu, L.; Varcoe, J. R.; Ong, A. L.; Poynton, S. D.; Xu, T. W., *J. Membr. Sci.* **2012**, *415*, 242-249.

34. Li, N. W.; Yan, T. Z.; Li, Z.; Thurn-Albrecht, T.; Binder, W. H., *Energ. Environ. Sci.* **2012**, *5*, 7888-7892.
35. Wang, J. H.; Li, S. H.; Zhang, S. B., *Macromolecules* **2010**, *43*, 3890-3896.
36. Gu, S.; Cai, R.; Luo, T.; Chen, Z. W.; Sun, M. W.; Liu, Y.; He, G. H.; Yan, Y. S., *Angew. Chem. Int. Ed.* **2009**, *48*, 6499-6502.



Cellulose nanocrystal-based composite electrolyte exhibited superior dimensional stability, handleability, and hydroxide conductivity.